Vietnam Journal of Mechanics, VAST, Vol. 32, No. 1 (2010), pp. 1 – 14

NON-LINEAR DYNAMICAL ANALYSIS OF IMPERFECT FUNCTIONALLY GRADED MATERIAL SHALLOW SHELLS

Dao Huy Bich, Vu Do Long
Vietnam National University, Hanoi

Abstract. Dynamical behaviors of functionally graded material shallow shells with geometrical imperfections are studied in this paper. The material properties are graded in the thickness direction according to the power-law distribution in terms of volume fractions of the constituents of the material. The motion, stability and compatibility equations of these structures are derived using the classical shell theory. The non-linear equations are solved by the Newmark's numerical integration method. The non-linear transient responses of cylindrical and doubly-curved shallow shells subjected to excited external forces are obtained and the dynamic critical buckling loads are evaluated based on the displacement responses using the criterion suggested by Budiansky and Roth. Obtained results show the essential influence of characteristics of functionally graded materials on the dynamical behaviors of shells.

1. INTRODUCTION

Functionally graded materials (FGM) as a new class of advanced inhomogeneous composite materials have received considerable attention in many engineering applications for improved structural efficiency in space structures and nuclear reactors since they were first reported in Japan [1].

In recent years important studies have been researched about the stability and vibration of functionally graded plates and cylindrical shells. Birman [2] presented a formulation of the stability problem for functionally graded hybrid composite plates subjected to uniaxial compression. Elastic bifurcation of functionally graded plates acted on by compressive loading was studied by Feldman and Aboudi [3]. Reddy et al [4] gave bending solution for functionally graded circular plates and annular plates. Woo and Meguid [5] presented an analytical solution for non-linear analysis of FGM plates and shallow cylindrical shells. Naj et al. [6] investigated FGM truncated conical shells under external pressure. Concerning with initial imperfections Sasam Shariat et al. [7] studied buckling problem of imperfect FGM plates under in-plane compressive loading.

About vibration of FGM plates Vel, Batra [8] gave three dimensional exact solution for the vibration of FGM rectangular plates; Ferreira et al [9] received natural frequencies of FGM plates by meshless method. Natural frequencies and buckling stresses of FGM plates were analyzed by Hiroyuki Matsunaga [10] using 2-D higher-order deformation theory. Pradhan et al [11] and Loy et al [12] studied vibration of FGM cylindrical shells

and the effects of boundary conditions and power law indices on the natural frequencies of these shells.

Research on the stability of FGM cylindrical shells under aperiodic axial impulse and dynamic torsional loading can be seen in the works of Sofiyev et al [13, 14]. Yang and Shen [15], Shen [16] gave a large deflection and post-buckling analysis of FGM plates and cylindrical shells subjected to various loadings.

Non-linear buckling analysis of FGM shallow spherical shells under pressure loads was presented by Ganapathi [17] by using finite element method, geometric non-linearity is assumed only on the meridional direction in strain-displacement relations. Dao H. B. [18] studied this problem using the approximated analytical method, geometric non-linearity is assumed in all strain-displacement relations.

The present research is concerned with non-linear dynamical analysis, including non-linear dynamical buckling analysis and non-linear vibration of functionally graded material shallow shells with initial imperfections. Derivations of governing equations of these shells are based on the shell theory according to the von Karman theory for moderately large deflection and small strain with the assumption of power law composition for the constituent materials. The non-linear transient responses of FGM cylindrical and doubly-curved shallow shells subjected to excited external loads are considered. The solution of dynamic problems is posed as the determination of dynamic critical buckling loads for various loading cases using here the criterion suggested by Budiansky and Roth. The influence of characteristics of functionally graded materials and initial imperfections on the dynamical behaviors of shells is to be investigated.

2. GOVERNING EQUATIONS

2.1. Functionally graded material (FGM)

FGMs are microscopically inhomogeneous materials, in which the material properties vary smoothly and continuously from one surface of the material to the other surface. These materials are made from a mixture of ceramic and metal, or a combination of different materials. For example, a functionally graded material may consist of stainless steel SUS 304 (metal with characteristics E= 201.04×10^9 N/m^2, $\nu = 0.3262$, $\rho = 8166$ kg/m^3) and zirconia ZrO_2(ceramic: $E = 244.27\times10^9$ N/m^2, $\nu = 0.2882$, ρ= 5700 kg/m^3), or consist of aluminum Al(metal: $E = 70\times10^9$ N/m^2, $\nu = 0.3$, $\rho = 2702$ kg/m^3) and alumina Al_2O_3 (ceramic: $E = 380\times10^9$ N/m^2, $\nu = 0.3$, $\rho = 3800$ kg/m^3). A such mixture of ceramic and metal with a continuously varying volume fraction can be manufactured. Especially FGM thin-walled structures with metal in inner surface and ceramic in outer surface are widely used in practice. Assume that [19] the modulus of elasticity E and the mass density ρ change in the thickness direction z, while the Poisson ratio ν is assumed to be constant. Denote V_m and V_c being volume-fractions of the metal and ceramic phases respectively, which are related by $V_m + V_c = 1$ and V_c is expressed as $V_c(z) = \left(\dfrac{2z+h}{2h}\right)^k$, where h is the thickness of thin-walled structure, k is the volume-fraction exponent ($k \geq 0$). Then the elasticity modulus, the mass density and the Poisson ratio of a functionally graded

material can be evaluated as following

$$\begin{aligned} E(z) &= E_m V_m + E_c V_c = E_m + (E_c - E_m)\left(\frac{2z+h}{2h}\right)^k, \\ \rho(z) &= \rho_m V_m + \rho_c V_c = \rho_m + (\rho_c - \rho_m)\left(\frac{2z+h}{2h}\right)^k, \\ \nu(z) &= \nu = \text{const}. \end{aligned} \tag{1}$$

The values with subscripts m and c belong to metal and ceramic respectively.

2.2. Functionally graded shallow shells

Shallow shells are assumed to have a relative small rise as compared with their spans. A rectangular shallow shell made of FGM is considered here. Let the (x_1, x_2) plane of the Cartesian coordinates overlap the rectangular plane area of the shell. The middle surface of the shell generally is defined in terms of curvilinear coordinates, but for the shallow shell the Cartesian coordinates can replace the curvilinear coordinates on the middle surface. Suppose that the FGM shallow shell of thickness h and in-plane edges a and b is subjected to a transverse load of intensity q_0 and compressive edge loads of intensities r_0 and p_0.

The non-linear strain-displacement relationships based upon the von Karman theory for moderately large deflection and small strain are

$$\begin{aligned} \varepsilon_1^0 &= \frac{\partial u}{\partial x_1} - k_1 w + \frac{1}{2}\left(\frac{\partial w}{\partial x_1}\right)^2, \quad \chi_1 = \frac{\partial^2 w}{\partial x_1^2}, \\ \varepsilon_2^0 &= \frac{\partial v}{\partial x_2} - k_2 w + \frac{1}{2}\left(\frac{\partial w}{\partial x_2}\right)^2, \quad \chi_2 = \frac{\partial^2 w}{\partial x_2^2}, \\ \gamma_{12}^0 &= \frac{\partial u}{\partial x_2} + \frac{\partial v}{\partial x_1} + \frac{\partial w}{\partial x_1}\cdot\frac{\partial w}{\partial x_2}, \quad \chi_{12} = \frac{\partial^2 w}{\partial x_1 \partial x_2} \quad , \end{aligned} \tag{2}$$

The strains are related in the compatibility equation

$$\frac{\partial^2 \varepsilon_1^0}{\partial x_2^2} + \frac{\partial^2 \varepsilon_2^0}{\partial x_1^2} - \frac{\partial^2 \gamma_{12}^0}{\partial x_1 \partial x_2} = \left(\frac{\partial^2 w}{\partial x_1 \partial x_2}\right)^2 - \frac{\partial^2 w}{\partial x_1^2}\cdot\frac{\partial^2 w}{\partial x_2^2} - k_1\frac{\partial^2 w}{\partial x_2^2} - k_2\frac{\partial^2 w}{\partial x_1^2} \quad . \tag{3}$$

The constitutive stress-strain equations for the shell material are omitted here for brevity, note however that the Young modulus $E(z)$ and the mass density $\rho(z)$ are power functions of z described by expressions (1). Integrating the stress-strain equations and their moments through the thickness of the shell we obtain the expressions of internal forces and moments resultants

$$\begin{aligned} N_1 &= \frac{E_1}{1-\nu^2}\left(\varepsilon_1^0 + \nu\varepsilon_2^0\right) - \frac{E_2}{1-\nu^2}\left(\chi_1 + \nu\chi_2\right), \\ N_2 &= \frac{E_1}{1-\nu^2}\left(\varepsilon_2^0 + \nu\varepsilon_1^0\right) - \frac{E_2}{1-\nu^2}\left(\chi_2 + \nu\chi_1\right), \\ N_{12} &= \frac{E_1}{2(1+v)}\gamma_{12}^0 - \frac{E_2}{1+\nu}\chi_{12}, \end{aligned} \tag{4}$$

or inversely

$$\begin{aligned}&\varepsilon_1^0=\frac{1}{E_1}\left(N_1-\nu N_2\right)+\frac{E_2}{E_1}\chi_1,\quad \varepsilon_2^0=\frac{1}{E_1}\left(N_2-\nu N_1\right)+\frac{E_2}{E_1}\chi_2,\\&\gamma_{12}^0=\frac{2(1+\nu)}{E_1}N_{12}+\frac{2E_2}{E_1}\chi_{12}.\end{aligned}\tag{5}$$

And

$$\begin{aligned}&M_1=\frac{E_2}{E_1}N_1-\frac{E_1E_3-E_2^2}{E_1(1-\nu^2)}\left(\chi_1+\nu\chi_2\right),\quad M_2=\frac{E_2}{E_1}N_2-\frac{E_1E_3-E_2^2}{E_1(1-\nu^2)}\left(\chi_2+\nu\chi_1\right)\\&M_{12}=\frac{E_2}{E_1}N_{12}-\frac{E_1E_3-E_2^2}{E_1(1+\nu)}\chi_{12},\end{aligned}\tag{6}$$

where

$$\begin{aligned}&E_1=\left(E_m+\frac{E_c-E_m}{k+1}\right)h,\quad E_2=\frac{\left(E_c-E_m\right)kh^2}{2\left(k+1\right)\left(k+2\right)},\\&E_3=\left[\frac{E_m}{12}+\left(E_c-E_m\right)\left(\frac{1}{k+3}-\frac{1}{k+2}+\frac{1}{4k+4}\right)\right]h^3.\end{aligned}$$

According to Love's theory the equations of motion are

$$\begin{aligned}&\frac{\partial N_1}{\partial x_1}+\frac{\partial N_{12}}{\partial x_2}=\rho_1\frac{\partial^2u}{\partial t^2},\quad \frac{\partial N_{12}}{\partial x_1}+\frac{\partial N_2}{\partial x_2}=\rho_1\frac{\partial^2v}{\partial t^2},\\&\frac{\partial^2M_1}{\partial x_1^2}+2\frac{\partial M_{12}}{\partial x_1\partial x_2}+\frac{\partial^2M_2}{\partial x_2^2}+\frac{\partial}{\partial x_1}\left(N_1\frac{\partial w}{\partial x_1}+N_{12}\frac{\partial w}{\partial x_2}\right)\\&+\frac{\partial}{\partial x_2}\left(N_{12}\frac{\partial w}{\partial x_1}+N_2\frac{\partial w}{\partial x_2}\right)+k_1N_1+k_2N_2+q_0=\rho_1\frac{\partial^2w}{\partial t^2},\end{aligned}\tag{7}$$

where $\rho_1=\int\limits_{-h/2}^{h/2}\rho(z)dz=\left(\rho_m+\dfrac{\rho_c-\rho_m}{k+1}\right)h.$

By taking the inertia forces $\rho_1\dfrac{\partial^2u}{\partial t^2}\to 0$ and $\rho_1\dfrac{\partial^2v}{\partial t^2}\to 0$ into consideration because of $u << w$, $v << w$, equations (7) and (8) are satisfied indentically by introducing the stress function φ

$$N_1=\frac{\partial^2\varphi}{\partial x_2^2};\quad N_2=\frac{\partial^2\varphi}{\partial x_1^2};\quad N_{12}=-\frac{\partial^2\varphi}{\partial x_1\partial x_2}.\tag{8}$$

and the equation (7) can be rewritten as

$$\begin{aligned}&\frac{\partial^2M_1}{\partial x_1^2}+2\frac{\partial M_{12}}{\partial x_1\partial x_2}+\frac{\partial^2M_2}{\partial x_2^2}+N_1\frac{\partial^2w}{\partial x_1^2}+2N_{12}\frac{\partial^2w}{\partial x_1\partial x_2}+N_2\frac{\partial^2w}{\partial x_2^2}+\\&k_1N_1+k_2N_2+q_0=\rho_1\frac{\partial^2w}{\partial t^2}.\end{aligned}\tag{9}$$

The substitution of equations (5) into the compatibility equation (3) and equations (6) into the motion equation (9), taking into account relations (8) yields a system of

equations in terms of the stress function φ and the deflection w

$$\frac{1}{E_1}\Delta\Delta\varphi = -k_1\frac{\partial^2 w}{\partial x_2^2} - k_2\frac{\partial^2 w}{\partial x_1^2} + \left(\frac{\partial^2 w}{\partial x_1 \partial x_2}\right)^2 - \frac{\partial^2 w}{\partial x_1^2}\frac{\partial^2 w}{\partial x_2^2}. \tag{10}$$

$$\begin{aligned}&\rho_1\frac{\partial^2 w}{\partial t^2} + \frac{E_1E_3 - E_2^2}{E_1(1-\nu^2)}\Delta\Delta w + 2\frac{\partial^2\varphi}{\partial x_1\partial x_2}\frac{\partial^2 w}{\partial x_1\partial x_2} - \frac{\partial^2\varphi}{\partial x_2^2}\frac{\partial^2 w}{\partial x_1^2} - \frac{\partial^2\varphi}{\partial x_1^2}\frac{\partial^2 w}{\partial x_2^2}\\ &-k_2\frac{\partial^2\varphi}{\partial x_1^2} - k_1\frac{\partial^2\varphi}{\partial x_2^2} = q_0.\end{aligned} \tag{11}$$

The initial imperfection of the shell considered here can be seen as a small deviation of the shell middle surface from the perfect shape, also seen as an initial deflection which is very small compared with the shell dimensions, but may be compared with the shell wall thickness. Let $w_0(x_1,x_2)$ denote a known small imperfection, proceeding from the motion equations (10) and (11) of a perfect FGM shallow shell and following to the Volmir's approach [20] for an imperfect shell we can formulate the system of motion equations for an imperfect FGM shallow shell as

$$\begin{aligned}&\frac{1}{E_1}\Delta\Delta\varphi = -k_1\frac{\partial^2(w-w_0)}{\partial x_2^2} - k_2\frac{\partial^2(w-w_0)}{\partial x_1^2} + \left[\left(\frac{\partial^2 w}{\partial x_1\partial x_2}\right)^2 - \frac{\partial^2 w}{\partial x_1^2}\frac{\partial^2 w}{\partial x_2^2}\right] -\\ &\left[\left(\frac{\partial^2 w_0}{\partial x_1\partial x_2}\right)^2 - \frac{\partial^2 w_0}{\partial x_1^2}\frac{\partial^2 w_0}{\partial x_2^2}\right] = 0,\end{aligned} \tag{12}$$

$$\begin{aligned}&\rho_1\frac{\partial^2 w}{\partial t^2} + \frac{E_1E_3 - E_2^2}{E_1(1-\nu^2)}\Delta\Delta(w-w_0) + 2\frac{\partial^2\varphi}{\partial x_1\partial x_2}\frac{\partial^2 w}{\partial x_1\partial x_2} - \frac{\partial^2\varphi}{\partial x_2^2}\frac{\partial^2 w}{\partial x_1^2} - \frac{\partial^2\varphi}{\partial x_1^2}\frac{\partial^2 w}{\partial x_2^2}\\ &-k_2\frac{\partial^2\varphi}{\partial x_1^2} - k_1\frac{\partial^2\varphi}{\partial x_2^2} = q_0.\end{aligned} \tag{13}$$

3. NON-LINEAR DYNAMICAL ANALYSIS

Suppose that the functionally graded shallow shell is simply supported at its edges and subjected to a transverse load $q_0(t)$ compressive edge loads $r_0(t)$ and $p_0(t)$. The boundary conditions can be expressed as

$$\begin{aligned}&w = 0, \quad M_1 = 0, \quad N_1 = -r_0h, \quad N_{12} = 0 \quad \text{at} \quad x_1 = 0; \quad x_1 = a,\\ &w = 0, \quad M_2 = 0, \quad N_2 = -p_0h, \quad N_{12} = 0 \quad \text{at} \quad x_2 = 0; \quad x_2 = b,\end{aligned} \tag{14}$$

where a and b are the lengths of in-plane edges of the shallow shell.

The mentioned conditions (14) can be satisfied if the deflection w and the stress function φ are represented by

$$w = f(t)\sin\frac{m\pi x_1}{a}\sin\frac{n\pi x_2}{b}, \quad \varphi = \eta(t)\left[\sin\frac{m\pi x_1}{a}\sin\frac{n\pi x_2}{b} - \theta(x_1) - \lambda(x_2)\right], \tag{15}$$

where f is the maximum deflection, $\theta(x_1)$, $\lambda(x_2)$ are chosen such that

$$\eta\theta''(x_1) = p_0h \quad , \quad \eta\lambda''(x_2) = r_0h \quad .$$

Concerning with the initial-imperfection $w_0(x_1, x_2)$ we introduce an assumption, it has the form like the shell deflection, i.e.

$$w_0(x_1, x_2) = f_0 \sin\frac{m\pi x_1}{a} \sin\frac{n\pi x_2}{b}, \tag{16}$$

where f_0 is a given constant.

Substituting expression (15), (16) in to equations (12), (13) and applying Bubnov-Galerkin procedure yield a set of two equations with respect to $f(t)$ and $\eta(t)$

$$\begin{aligned}
&\frac{1}{E_1}\left(m^2 + n^2\lambda^2\right)^2 \eta - \frac{a^2}{\pi^2}\left(k_1 n^2\lambda^2 + k_2 m^2\right)(f - f_0) + \frac{16mn}{3\pi^2}\left(f^2 - f_0^2\right) = 0,\\
&\rho_1 \frac{d^2 f}{dt^2} + \frac{(E_1E_3 - E_2^2)}{E_1(1-\nu^2)} \frac{\left(m^2 + n^2\lambda^2\right)^2 \lambda^4}{a^4}(f - f_0) + \frac{\pi^2}{a^2}\left(k_1 n^2\lambda^2 + k_2 m^2\right)\eta -\\
&- \frac{\pi^2 h}{a^2}\left(m^2 r_0 + n^2\lambda^2 p_0\right) - \frac{32mn\lambda^2\pi^2}{3a^4} f\eta + \frac{16h}{\pi^2 mn}\left(k_1 r_0 + k_2 p_0\right) = \frac{16q_0}{\pi^2 mn},
\end{aligned}$$

where $\lambda = \dfrac{a}{b}$.

Eliminating η from two obtained equations leads to a non-linear second-order ordinary differential equation for $f(t)$.

$$\begin{aligned}
&\rho_1 \frac{d^2 f}{dt^2} + \left[\frac{(E_1E_3 - E_2^2)}{E_1(1-\nu^2)} \frac{\left(m^2 + n^2\lambda^2\right)\pi^4}{a^4} + \frac{E_1\left(k_1 n^2\lambda^2 + k_2 m^2\right)^2}{\left(m^2 + n^2\lambda^2\right)^2}\right](f - f_0)\\
&- \frac{16E_1 mn\lambda^2(k_1 n^2\lambda^2 + k_2 m^2)}{3a^2(m^2+n^2\lambda^2)^2}[f^2 - f_0^2 + 2f(f - f_0)] + \frac{512E_1 m^2 n^2\lambda^4}{9a^4(m^2+n^2\lambda^2)^2} f(f^2 - f_0^2)\\
&- \frac{\pi^2 h}{a^2}\left(m^2 r_0 + n^2\lambda^2 p_0\right) f + \frac{16h}{\pi^2 mn}\left(k_1 r_0 + k_2 p_0\right) = \frac{16q_0}{\pi^2 mn}
\end{aligned} \tag{17}$$

The obtained equation (17) is a governing equation for dynamic analysis of imperfect functionally graded doubly-curved shallow shells in general. Based on this equation the non-linear vibration of perfect and imperfect FGM shallow shells can be investigated and the post-buckling analysis of shells under various loading cases can be performed. Particularly for a spherical panel we put $k_1 = k_2$ in the equation (17), for a cylindrical shell $k_1 = 0$ and for a plate $k_1 = k_2 = 0$. Combined with the equation (17) for obtaining the non-linear dynamic response the initial conditions are assumed as $f(0) = f_0$, $\dot{f}(0) = 0$. The applied loads are varying as functions of time. The non-linear equation (17) is solved by the Newmark's numerical integration method. Equilibrium is achieved for each time step through direct iteration until the chosen convergence criteria are satisfied.

By use of Eq. (17) we consider two aspects: vibration characteristics and dynamical stability characteristics of FGM shallow shells.

3.1. Non-linear vibration of FGM shallow shells

Consider an imperfect functionally graded shallow shell acted on by an uniformly distributed excited transverse load $q_0(t) = Q\sin\Omega t$, i.e. $r_0 = p_0 = 0$ the equation of

motion (17) has of the form

$$\rho_1 \frac{d^2 f}{dt^2} + \left[\frac{(E_1 E_3 - E_2^2)}{E_1(1-\nu^2)} \frac{\left(m^2 + n^2\lambda^2\right)\pi^4}{a^4} + \frac{E_1\left(k_1 n^2\lambda^2 + k_2 m^2\right)^2}{\left(m^2 + n^2\lambda^2\right)^2} \right] (f - f_0)$$
$$- \frac{16 E_1 mn\lambda^2 \left(k_1 n^2\lambda^2 + k_2 m^2\right)}{3a^2\left(m^2 + n^2\lambda^2\right)^2} \left[f^2 - f_0^2 + 2f(f - f_0)\right] \tag{18}$$
$$+ \frac{512 E_1 m^2 n^2 \lambda^4}{9a^4\left(m^2 + n^2\lambda^2\right)^2} f\left(f^2 - f_0^2\right) = \frac{16Q\sin\Omega t}{\pi^2 mn}.$$

From Eq.(18) the fundamental frequencies of natural vibration of the shell can be determined by the relation

$$\omega_{mn}^2 = \frac{1}{\rho_1}\left[\frac{(E_1 E_3 - E_2^2)}{E_1(1-\nu^2)} \frac{\left(m^2 + n^2\lambda^2\right)\pi^4}{a^4} + \frac{E_1\left(k_1 n^2\lambda^2 + k_2 m^2\right)^2}{\left(m^2 + n^2\lambda^2\right)^2} \right] . \tag{19}$$

The FGM shallow shells considered here are a spherical panel with in-plane edges $a = b = 2$ m; $h = 0.01$ m; $k_1 = k_2 = \dfrac{1}{R}$ (with $R = 5m$) and a cylindrical panel $a = b = 2$ m; $h = 0.01$ m; $k_1 = 0$; $k_2 = \dfrac{1}{R}$ (with R= 5 m). The shells are simply supported at all its edges. The combination of materials consists of aluminum ($E_m = 70.10^9$ N/m^2 ; $\rho_m =$ 2702 kg/m^3) and alumina ($E_c = 380.10^9$ N/m^2; $\rho_c = 3800$ kg/m^3). The Poisson ratio is chosen to be 0.3 for simplicity.

Four first natural frequencies of FGM spherical panel are shown in the tables 1a (with $\lambda = \dfrac{a}{b} = 1$) and 1b (with $\lambda = \dfrac{a}{b} = 2$)

Table 1a

k \ (m,n)	(1,1)	(3,1)	(1,3)	(3,3)
k=0	2005	2135	2135	2410
k=1	1667	1758	1758	1954
k=2	1506	1590	1590	1769

Table 1b

k \ (m,n)	(1,1)	(3,1)	(1,3)	(3,3)
k=0	2304	2223	3410	3910
k=1	1688	1821	2686	3057
k=2	1525	1647	2436	2774

The table 2a and 2b represent four first natural frequencies of FGM cylindrical panel with $\lambda = 1$ and $\lambda = 2$ respectively.

Obviously the natural frequencies of FGM shallow shells are observed to be dependent on the constituent volume fractions, they decrease when increasing the power law index k. When $k = 0$, representing full ceramic shell, the natural frequencies are considerably greater than frequencies of FGM shells. The reason is the higher value of the assumed modulus of elasticity of the ceramic constituent.

Table 2a

k \ (m,n)	(1,1)	(3,1)	(1,3)	(3,3)
k=0	1011	1948	773	1675
k=1	839	1602	593	1302
k=2	758	1448	539	1197

Table 2b

k \ (m,n)	(1,1)	(3,1)	(1,3)	(3,3)
k=0	547	1690	2763	3383
k=1	438	1369	2109	2586
k=2	396	1239	1917	2351

For obtaining the non-linear transient responses of FGM shells acted on by the harmonic uniformly load $q_0(t) = Q \sin \Omega t$, the equation (18) is solved by using the Newmark procedure and direct iteration method. The time-step Δt is taken as $T/300$ where period $T = 2\pi/\Omega$, Ω is the frequency of excited load and $t_n = n\Delta t$.

Fig. 1 shows non-linear responses of perfect functionally graded spherical shell with different power law indices subjected to excited load of magnitude $Q = 150.000 \quad (N/m^2)$ and frequency $\Omega = 1000 \quad (s^{-1})$

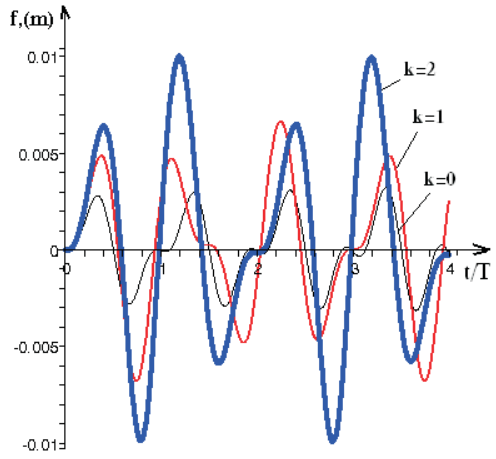

Fig. 1. Non-linear transient responses of FGM spherical panel with various k

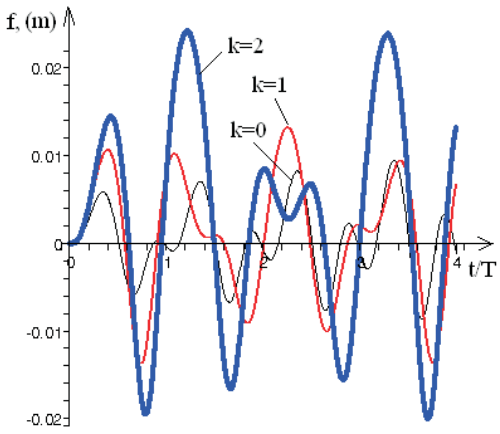

Fig. 2. Non-linear transient responses of FGM cylindrical panel with various k

Non-linear transient responses of FGM cylindrical panel subjected to transverse excited load $q_0(t) = 15.000 \sin 500t$ are presented on the Fig. 2.

Fig. 3 shows the influence of initial imperfection amplitude $f_0 = 10^{-1}h$ on the non-linear responses of FGM spherical panel with power law index $k = 1$ under excited load $q_0(t) = 75.000 \sin 1650t$.

From obtained results one can see that frequencies of non-linear vibration of FGM shallow shells decrease, while amplitudes increase, when increasing the power law indices, the non-linear transient responses perform the phenomenon like periodic cycles. The initial

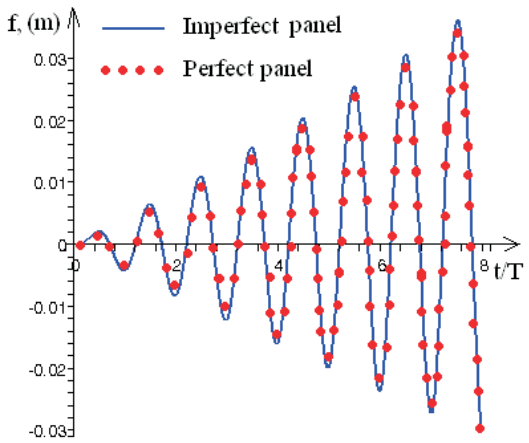

Fig. 3. Influence of initial imperfection on non-linear responses.

imperfection $f_0 = 10^{-1}h$ has a slight influence on the non-linear responses of the considered FGM spherical panel.

3.2. Non-linear dynamical buckling analysis of FGM shallow shells

Investigate the non-linear dynamic buckling of imperfect functionally graded spherical and cylindrical panels in some cases of active loads varying as linear functions of time. The aim of considered problems is to search the critical dynamic buckling loads. They can be evaluated based on the displacement responses obtained from the motion equation (17). The criterion suggested by Budiansky and Roth is employed here as it is widely accepted. This criterion is based on that, for large values of loading speed the amplitude-time curve of obtained displacement response increases sharply depending on time and this curve obtains a maximum by passing from the slope point, and at the time $t = t_{cr}$ a stability loss occurs. Here $t = t_{cr}$ is called critical time and the load corresponding to this critical time is called dynamic critical buckling load.

3.2.1. *Imperfect FGM cylindrical panel acted on by axial compressive load.*

The equation (17) in this case $k_1 = 0$, $k_2 = \dfrac{1}{R}$, $p_0 = q_0 = 0$ can be rewritten as

$$\begin{aligned}
&\rho_1 \frac{d^2 f}{dt^2} + \left[\frac{(E_1 E_3 - E_2^2)}{E_1(1-\nu^2)} \frac{\left(m^2 + n^2\lambda^2\right)\pi^4}{a^4} + \frac{E_1 m^4}{R^2\left(m^2 + n^2\lambda^2\right)^2} \right] (f - f_0) \\
&- \frac{16 E_1 m^3 n \lambda^2}{3Ra^2(m^2 + n^2\lambda^2)^2} [f^2 - f_0^2 + 2f(f - f_0)] \\
&+ \frac{512 E_1 m^2 n^2 \lambda^4}{9a^4(m^2 + n^2\lambda^2)^2} f(f^2 - f_0^2) - \frac{\pi^2 h m^2 r_0}{a^2} f = 0.
\end{aligned} \tag{20}$$

The static critical load can be determined by the equation to be reduced from Eq. (20) by putting $\ddot{f} = 0$, $f_0 = 0$

$$\frac{\pi^2 h m^2 r_0}{a^2} f = \left[\frac{(E_1 E_3 - E_2^2)}{E_1(1-\nu^2)} \frac{\left(m^2 + n^2\lambda^2\right)\pi^4}{a^4} + \frac{E_1 m^4}{R^2 \left(m^2 + n^2\lambda^2\right)^2} \right] f -$$
$$- \frac{16 E_1 m^3 n \lambda^2}{3Ra^2 \left(m^2 + n^2\lambda^2\right)^2} f^2 + \frac{512 E_1 m^2 n^2 \lambda^4}{9a^4 \left(m^2 + n^2\lambda^2\right)^2} f^3.$$

Taking $f \neq 0$, i.e. considering the shell after the loss of stability we obtain

$$\frac{\pi^2 h m^2 r_0}{a^2} = \frac{(E_1 E_3 - E_2^2)}{E_1(1-\nu^2)} \frac{\left(m^2 + n^2\lambda^2\right)\pi^4}{a^4} + \frac{E_1 m^4}{R^2 \left(m^2 + n^2\lambda^2\right)^2} -$$
$$- \frac{16 E_1 m^3 n \lambda^2}{3Ra^2 \left(m^2 + n^2\lambda^2\right)^2} f + \frac{512 E_1 m^2 n^2 \lambda^4}{9a^4 \left(m^2 + n^2\lambda^2\right)^2} f^2. \tag{21}$$

From Eq. (21) the upper buckling load can be determined by putting $f = 0$

$$r_{upper} = \frac{a^2}{\pi^2 h m^2} \left[\frac{(E_1 E_3 - E_2^2)}{E_1(1-\nu^2)} \frac{\left(m^2 + n^2\lambda^2\right)\pi^4}{a^4} + \frac{E_1 m^4}{R^2 \left(m^2 + n^2\lambda^2\right)^2} \right]$$

and the lower buckling load is found using the condition $\frac{dr_0}{df} = 0$, it follows

$$r_{\text{lower}} = \frac{a^2}{\pi^2 h m^2} \left[\frac{(E_1 E_3 - E_2^2)}{E_1(1-\nu^2)} \frac{\left(m^2 + n^2\lambda^2\right)\pi^4}{a^4} - \frac{E_1 m^4}{8R^2 \left(m^2 + n^2\lambda^2\right)^2} \right].$$

The cylindrical panel considered here is made of the same functionally graded material aluminum / alumina and subjected to axial compressive load varying linearly on time as $r_0 = st$. The imperfection amplitude is taken as $f_0 = 10^{-2}h$, the curvature of panel $k_2 = \frac{1}{5}(m^{-1})$, $a = 2m$, and the dimension ratio $\lambda = 1$

Fig 4. shows the effect of buckling mode shapes on load-deflection curve of FGM cylindrical panel with the power law index $k = 1$ under compressive load $r_0 = 1,5.10^9 t$. Clearly, the smallest critical dynamic buckling load corresponds to the buckling mode shape $m = 3$, $n = 1$ and is equal to value $r_{cr} = 3,8.10^8 N/m^2$.

The effect of power law indices k on load-deflection curve is illustrated in the Fig.5, from that we obtain dynamic critical buckling load $r_{cr} = 6,375.10^8 N/m^2$(for $k = 0$) , $r_{cr} = 3,8.10^8 N/m^2$ (for $k = 1$) , $r_{cr} = 3,0.10^8 N/m^2$ (for $k = 2$) respectively. The critical dynamic buckling load decreases when increasing the power law index k. The full ceramic shell (with $k = 0$) has the greatest dynamic critical buckling load .

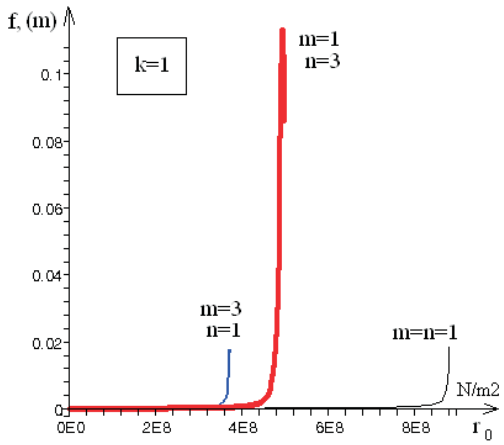

*Fig. 4.*Effect of buckling mode shapes on load-deflection curve

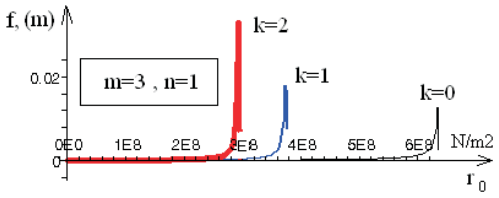

Fig. 5. Effect of power law index k on load-deflection curve

3.2.2. *Imperfect FGM cylindrical panel subjected to transverse load*

In this case $k_1 = 0$; $k_2 = \dfrac{1}{R}$, $p_0 = r_0 = 0$ the motion equation (17) has the form

$$\rho_1 \frac{d^2 f}{dt^2} + \left[\frac{(E_1 E_3 - E_2^2)}{E_1(1-\nu^2)} \frac{\left(m^2 + n^2\lambda^2\right)\pi^4}{a^4} + \frac{E_1 m^4}{R^2\left(m^2 + n^2\lambda^2\right)^2} \right](f - f_0)$$
$$- \frac{16E_1 m^3 n\lambda^2}{3Ra^2(m^2+n^2\lambda^2)^2}[f^2 - f_0^2 + 2f(f-f_0)] + \frac{512E_1 m^2 n^2 \lambda^4}{9a^4(m^2+n^2\lambda^2)^2} f(f^2 - f_0^2) = \frac{16q_0}{\pi^2 mn}. \tag{22}$$

The static critical load can be determined from Eq.(22) by putting $\ddot{f} = 0$, $f_0 = 0$ and using condition $\dfrac{dq_0}{df} = 0$.

The FGM cylindrical panel considered here is the same as mentioned in the previous section (i), but under uniformly transverse load varying on time as $q_0 = 10^6 t$. It is found that the smallest critical dynamic buckling load corresponds to the buckling mode shape $m = n = 1$ and is equal to $q_0 = 0.2233 \times 10^6$ N/m^2 (see Fig.6). The critical buckling load for the FGM cylindrical panel with power law index $k = 1$ and $\lambda = 1$ under axial compression is greater than that under transverse load.

Fig. 7 demonstrates the effect of power law indices on load-deflection curve. The critical dynamic buckling load has the same tendency decreasing when increasing the power law index: $q_{cr} = 0.366 \times 10^6$ N/m^2 (for $k = 0$) ; $q_{cr} = 0.2233 \times 10^6$ N/m^2 (for $k = 1$) and $q_{cr} = 0.175 \times 10^6$ N/m^2 (for $k = 2$) .

Accordingly comparing with dynamic buckling analysis of perfect FGM cylindrical panel under transverse load we can see that the imperfection has a slight influence on the critical load.

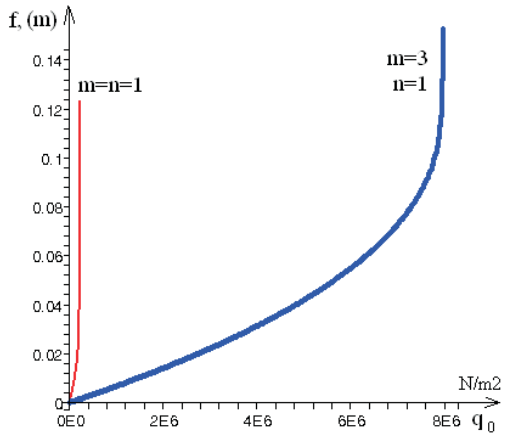

*Fig. 6.*Effect of buckling mode shapes on load-deflection curve

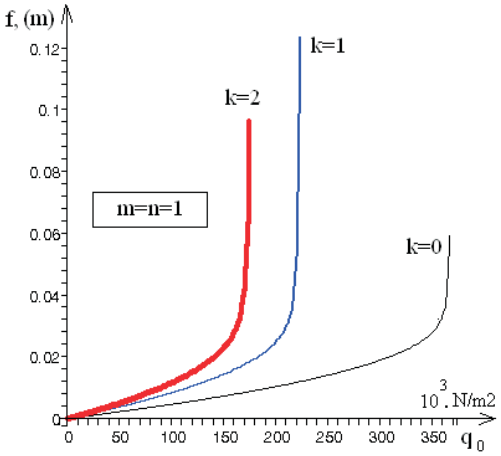

Fig. 7. Effect of power law indices on load-deflection curve

3.2.3. *Imperfect FGM spherical panel under transverse load*

The motion equation (17) in this case $k_1 = k_2 = \dfrac{1}{R}$, $p_0 = r_0 = 0$, is of the form

$$\rho_1 \frac{d^2 f}{dt^2} + \left[\frac{(E_1 E_3 - E_2^2)}{E_1(1-\nu^2)} \frac{\left(m^2 + n^2\lambda^2\right)\pi^4}{a^4} + \frac{E_1}{R^2} \right] (f - f_0)$$
$$- \frac{16 E_1 mn\lambda^2}{3Ra^2(m^2+n^2\lambda^2)}[f^2 - f_0^2 + 2f(f-f_0)] + \frac{512 E_1 m^2 n^2 \lambda^4}{9a^4(m^2+n^2\lambda^2)^2} f(f^2 - f_0^2) = \frac{16 q_0}{\pi^2 mn}. \tag{23}$$

Substituting $\ddot{f} = 0$ and $f_0 = 0$ into Eq.(23) and using condition $\dfrac{dq_0}{df} = 0$ we can determine the static critical load.

Consider a functionally graded spherical panel under transverse load varying on time as $q_0 = st$. Geometric characteristics of panel are: $a = 2m$, $h = 1cm$, $\lambda = 1$, $R = 5m$ and the imperfection amplitude $f_0 = 10^{-2}h$.

The effect of buckling mode shapes on load-deflection curve of the mentioned FGM spherical panel with the power law index $k = 1$ under transverse load $q_0 = 10^6 t$ is illustrated in the Fig.8. Obviously, the smallest critical dynamic buckling load corresponds to the buckling mode shape $m = 1$, $n = 1$ and is equal to value $q_{cr} = 1,628.10^6 N/m^2$

Fig. 9 shows the graphs of load-deflection curve of FGM spherical panel with various power law indices, from that to obtain $q_{cr} = 2.746 \times 10^6$ (N/m^2) (for $k = 0$), $q_{cr} = 1.628 \times 10^6$ (N/m^2) (for $k = 1$) and $q_{cr} = 1.258 \times 10^6$ (N/m^2) (for $k = 2$). The critical dynamic buckling loads of FGM spherical panel are found to be similar to those of FGM cylindrical panel. Comparing with results of perfect FGM spherical panel $q_{cr} = 2.751 \times 10^6$ (N/m^2) (for $k = 0$), $q_{cr} = 1.633 \times 10^6$ (N/m^2) and $q_{cr} = 1.26 \times 10^6$ (N/m^2) leads to a conclusion that the initial imperfection $f_0 = 10^{-2}h$ slightly influences on the critical dynamic buckling load.

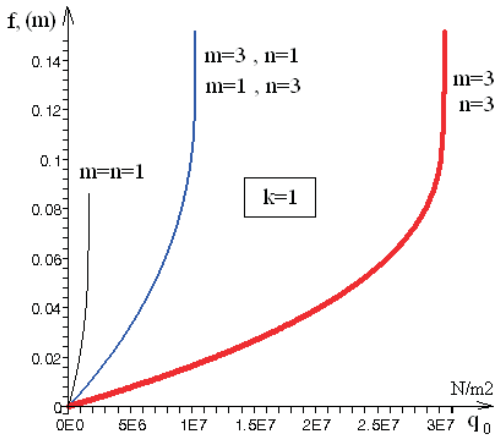

*Fig. 8.*Effect of buckling mode shapes on load-deflection curve

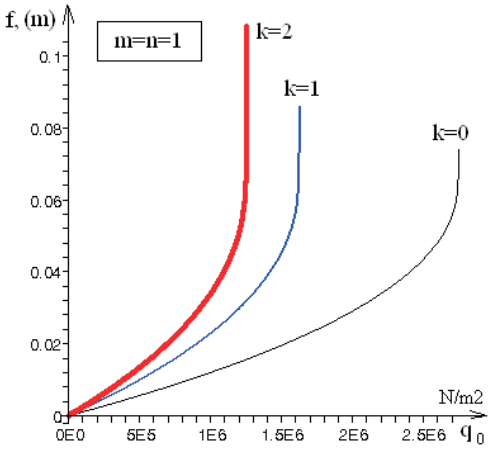

Fig. 9. Effect of power law index on load-deflection curve

4. CONCLUSION

The governing equations for non-linear dynamical analysis of functionally graded shallow shells, including geometric non-linearity, are derived. Derivations are based on the classical shell theory and with the assumption of power law composition for the constituent materials.

Non-linear vibration of FGM shallow shells is studied. Frequencies of non-linear vibration decrease, while amplitudes increase, when increasing the power law index, the non-linear transient responses perform the phenomenon like periodic cycles.

Non-linear dynamical buckling analysis of FGM shallow shells is carried out. Illustrating numerical results obtained here show that the critical dynamic buckling loads for FGM shallow shells decrease when increasing the power law index.

The initial imperfection has a slight influence on dynamical characteristics of FGM shallow shells.

ACKNOWLEDGEMENT

This work is completed with partly financial support of VNU project QGTD. 09. 01.

REFERENCES

[1] M. Koizumi, The concept of FGM, *Ceram. Trans. Funct. Grad. Mater.* **34** (1993) 3-10.
[2] V. Birman, Buckling of functionally graded hybrid composite plates, *Proc. of 10^{th} Conf. on Eng. Mech.* USA, 1995.
[3] E. Feldman, J. Aboudi, Buckling analysis of FGM plates subjected to uniaxial loading. *Composite Structures* **38** (1997) 29-36.
[4] J. N. Reddy et al, Axisymmetric bending of FGM circular and annular plates, *European J. of Mech.* **18** (1999) 185-199.

[5] J. Woo, S. A. Meguid, Non-linear analysis of FGM plates and shallow shells, *Int. J. Solid Struct.* **38** (2001) 7409-7421.
[6] R. Naj, M. Sabzikar, M. R. Eslami, Thermal and mechanical instability of FGM truncated conical shells, *Thin-walled Structures* **46** (2008) 65-78.
[7] B. A. Sasam Shariat, R. Javaheri, M.R. Eslami, Buckling of imperfect FGM plates under in-plane compressive loading, *Thin-walled Structures* **43** (2005) 1020-1036.
[8] S. S. Vel, R. C. Batra, Three dimensional exact solution for the vibration of FGM rectangular plates, *J. Sound and Vibration* **272** (3) (2004) 703-730.
[9] A. J. M. Ferreira, R. C. Batra, C. M. C. Roque, Natural frequencies of FGM plates by meshless method, *Composite Structures* **75** (2006) 593-600.
[10] Hiroyuki Matsunaga, Free vibration and stability of FGM plates according to a 2-D high order deformation theory, *Composite Structures* **82** (2008) 499-512.
[11] S. C. Pradhan, C. T. Loy, K. Y. Lam, J. N. Reddy, Vibration characteristics of FGM cylindrical shells under various boundary conditions, *Applied Acoustics* **61** (2000) 111-129.
[12] C. T. Loy, K. T. Lam, J. N. Reddy, Vibration of FGM cylindrical shells, *Int. J. Mech. Sei* **41** (1999) 309-324.
[13] A. H. Sofiyev, The stability of compositionally graded ceramic-metal cylindrical shells under aperiodic axial impulse loading, *Composite Structures* **69** (2005) 247-257.
[14] A. H. Sofiyev, E. Schnack, The stability of FGM cylindrical shells under linearly increasing dynamic torsional loading, *Engineering Structures* **26** (2004) 1321-1331.
[15] J. Yang, H. S. Shen, Non-linear analysis of FGM plates under transverse and in-plane loads, *Int. J. Non-linear Mech.* **38** (2003) 467-482.
[16] H. S. Shen, Post-buckling analysis of pressure-loaded FGM cylindrical shells in thermal environments, *Engineering Structures* **25** (2003) 487-497.
[17] M. Ganapathi, Dynamic stability characteristics of FGM shallow spherical shells, *Composite Structures* **79** (2007) 338-343.
[18] Dao Huy Bich, Non-linear buckling analysis of functionally graded shallow spherical shells, *Vietnam Journal of Mechanics* **31** (2009) 17-30.
[19] R. Javaheri, M. R. Eslami, Buckling of FGM plates subjected to temperature rise, *Proc. of* 4^{th} *Int. Congress on the thermal stresses*, Osaka Japan, June 8-11, 2001, 167-170.
[20] A. S. Volmir, *Non-linear dynamics of plates and shells*, Science Edition, M. 1972.

Received June 21, 2009

PHÂN TÍCH PHI TUYẾN ĐỘNG LỰC VỎ THOẢI KHÔNG HOÀN HẢO BẰNG VẬT LIỆU CÓ CƠ TÍNH BIẾN THIÊN

Trong bài báo này khảo sát các tính chất động lực của vỏ thoải không hoàn hảo bằng vật liệu có cơ tính biến thiên. Cơ tính của vật liệu biến thiên theo chiều dày của vỏ theo quy luật phân bố phụ thuộc vào thể tích thành phần của các vật liệu tham gia tạo thành vật liệu vỏ. Đã thiết lập các phương trình chuyển động, phương trình ổn định và phương trình tương thích của vỏ tính đến phi tuyến hình học. Giải các phương trình phi tuyến bằng phương pháp tích phân số Newmark. Đã nhận được đáp ứng phi tuyến tức thời của vỏ trụ và vỏ hai độ cong dưới tác dụng của lực kích động ngoài. Tải trọng động tới hạn của vỏ được xác định dựa trên tiêu chuẩn Budiansky-Roth. Các kết quả nhận được cho thấy ảnh hưởng đáng kể của các đặc trưng vật liệu cơ tính biến thiên đến các tính chất động lực của vỏ.